IR + Raman - IR- and Raman-Spectroscopy

Protocol for the PC 2 lab course by

Vincent Kümmerle & Elvis Gnaglo & Julian Brügger

University of Stuttgart

authors:	Vincent Kümmerle, 3712667 st187541@stud.uni-stuttgart.de
	Elvis Gnaglo, 3710504 st189318@stud.uni-stuttgart.de
	Julian Brügger, 3715444 st190050@stud.uni-stuttgart.de
group number:	A05
date of experiment:	21.01.2026
supervisor:	Mansha Shafquath
submission date:	January 27, 2026

Abstract:

Contents

1 Theory

1.1 IR-Spectroscopy

When a dipolar molecule is exposed to an electromagnetic field the partially positively charged atom is pushed along the direction of the electric field lines. So if a molecule is exposed to an oscillating field, that oscillates at the natural vibration frequency of said molecule, the molecule will be in an excited vibrational state. For a linear molecule, the amount of vibrational modes is calculated as described in Equation 1.[1]

$$3N - 5 \tag{1}$$

For non-linear molecules the number of vibrational modes is defined as described in Equation 2

$$3N - 6 \tag{2}$$

Where N is in either case the number of atoms.

1.1.1 Diatomic molecules

When looking at just diatomic molecules, only one type of vibration can be observed, the stretching vibration, which is, figuratively speaking, the two atoms moving towards and apart from each other. Furthermore this vibration can be approximated as a harmonic oscillation. The vibrational frequency ν can be derived based on Hooke's law as shown in Equation 3.

$$\nu = \frac{1}{2\pi}\sqrt{\frac{k}{\mu}} \tag{3}$$

The force constant of the chemical bond is defined as k in Equation 3, whereas the reduced mass μ is defined in Equation 4.

$$\mu = \frac{m_1 \cdot m_2}{m_1 + m_2} \tag{4}$$

1.1.2 Polyatomic molecules

In polyatomic molecules, multiple vibrational modes, depending on the geometry and the number of atoms, are possible. As described in chapter 1.1.2 stretching vibrations represent a change in interatomic distance along the bond axis. Those stretching vibrations can occur symmetrically or asymmetrically. The other category of vibrational modes is called deformation vibrations. During a deformation vibration, the angles of the bonds change, whereas the bond lengths don't change significantly. The four modes of deformation vibrations are Scissoring, where two atoms move toward or away from each other like scissor blades; Wagging, where the atoms move out and back into the plane; Rocking, where the atoms swing back and forth within the same plane; and finally, Twisting, where the atoms rotate around the bond axis.

1.2 The FTIR Spectrometer

The measurement is conducted using a Fourier Transform Infrared (FTIR) spectrometer, the schematic assembly of which is depicted in Figure 1. Central to this apparatus is a Michelson interferometer, which modulates the infrared light to allow specific wavelength patterns to interact with the sample before reaching the detector. The resulting data are presented as an IR spectrum, where the signal intensity is plotted as a function of the wavenumber. To derive this frequency-domain spectrum from the raw temporal data, a Fourier transformation is applied to the recorded interferogram, effectively resolving the individual spectral components.[1]

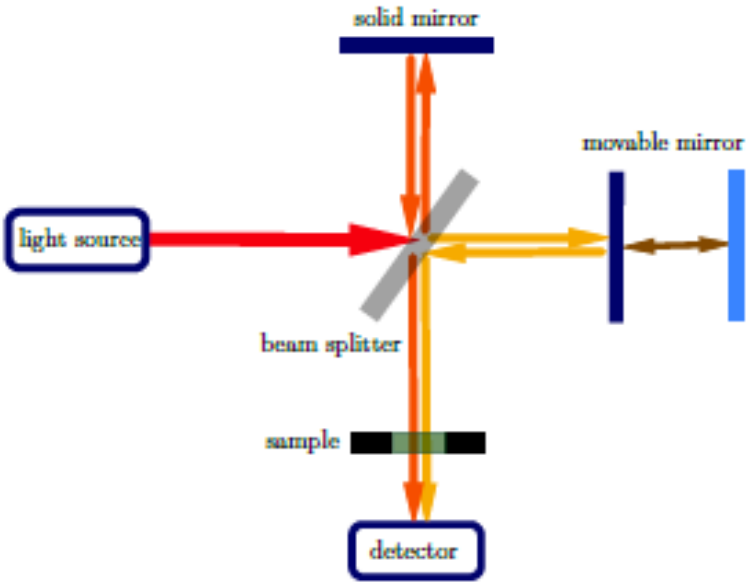

Fig. 1: Function of a FTIR spectrometer.[1]

To ensure a quick and non-destructive measurement, the ATR technique is used while the sample is placed on a crystal, which avoids the need for complex sample preparation.

1.3 Raman-Spectroscopy

1.3.1 Fundamental principle of Raman scattering

When a molecule interacts with the electric field of a light wave, its electron cloud is deformed. As a result of that deformation, a dipole $\vec{p}$ is induced. This dipole depends on the electric field vector $\vec{E}$ and the polarizability of the molecule α as portrayed in Equation 5.

$$\vec{p} = \alpha \cdot \vec{E} \tag{5}$$

Elastic and inelastic scattering can occur due to this process. During an elastic scattering process (Rayleigh scattering) the molecule absorbs the energy of the photon and emits that same amount of energy. During the inelastic Stokes scattering process, the molecule absorbs the energy of the photon, is excited to a virtual state and relaxes to a higher vibrational level than its initial state, resulting in a loss of photon energy. Conversely, there is also inelastic Anti-Stokes scattering, in which the molecule emits more energy than it originally absorbed. These three kinds of scattering are shown in Figure 2.

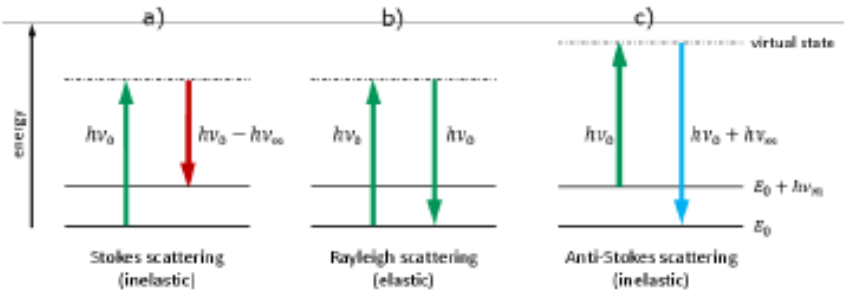

Fig. 2: Energy diagramms of the processes of a inelastic Stokes scattering, b elastic Rayleigh-Raman scattering and c inelastic Anti-Stokes scattering.[1]

1.3.2 The Raman spectrometer

In a Raman spectrometer, a laser serves as the monochromatic light source directed onto the sample, where the majority of photons undergo elastic Rayleigh scattering, while only a minute fraction is scattered inelastically. To isolate the Raman signal, the scattered light is directed through a diffraction grating that separates the different wavelengths before the intensity is captured by a detector. The resulting spectrum displays various Raman shifts, which represent the energy difference between the incident and scattered light. The schematic structure of the Raman-spectrometer used is displayed in Figure 3.[1]

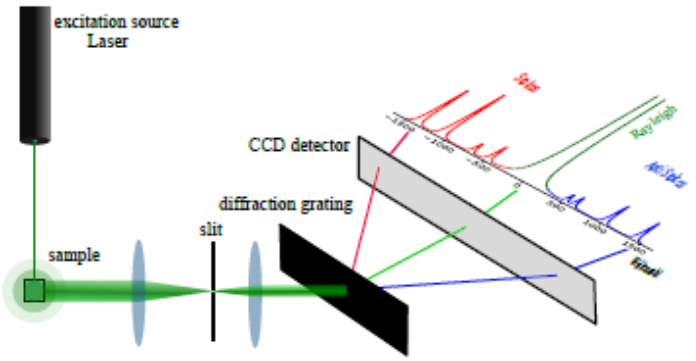

Fig. 3: Function of a Raman spectrometer.[1]

1.4 DFT-Calculations

To identify the various peaks in IR and Raman spectra, the theoretical values of each vibration are calculated via density functional theory (DFT). This quantum mechanical method is used due to its satisfactory compromise between short calculation times and precise values.[1]

2 Procedure

To simulate and calculate the vibrational normal modes, the program `Avogadro2` was used. The structures of the molecules methane, chloromethane, dichloromethane, dibromomethane, chloroform, deuterated chloroform, tetrachloromethane and tetrachloroethylene were built, their geometry was optimized and the optimized coordinates were used to calculate the vibrational modes with the `ORCA` software, resulting in a list of IR and Raman frequencies and intensities for each molecule.
In the experimental part, the Raman spectra of dichloromethane, dibromomethane, chloroform, deuterated chloroform, tetrachloromethane and tetrachloroethylene were measured and analysed with the `WPenlighten` software. The IR spectra of dichloromethane, dibromomethane, chloroform and tetrachloroethylene were measured using an ATR spectrometer and analysed with the `Opus` software.

3 Results and Analysis

3.1 Methane

3.1.1 IR

The simulated vibrational modes of methane are summarized in Table 1 with the corresponding wavenumber, intensity and vibration type of each mode.

Tab. 1: Listed are the simulated wavenumbers and intensities of the IR signals of CH_4 with the corresponding type of the vibrational mode.

Signal	Wavenumber $\tilde{\nu}$ / cm^{-1}	Intensity / $KM \cdot mol^{-1}$	Vibration type
1	1313.45	13.30	asym. bending
2	1313.68	13.25	asym. bending
3	1313.73	13.25	asym. bending
4	1530.79	0	sym. bending
5	1531.05	0	sym. bending
6	3019.38	0	sym. stretching
7	3152.03	17.69	asym. stretching
8	3152.33	17.64	asym. stretching
9	3152.45	17.64	asym. stretching

As can be seen in Table 1, only the asymmetric bending and stretching modes are IR-active, while the symmetric bending and stretching modes are IR-inactive. Furthermore, the asymmetric stretching mode shows the highest wavenumber among the IR-active modes, meaning it requires the most energy to be excited.

3.1.2 Raman

The simulated Raman-active vibrational modes of methane are summarized in Table 2 with the corresponding wavenumber, Raman intensity and vibration type of each mode.

Tab. 2: Listed are the simulated wavenumbers and intensities of the Raman signals of CH_4 with the corresponding type of the vibrational mode.

Mode	Raman shift $\Delta\tilde{\nu}$ / cm^{-1}	Raman intensity / $Å^4 \cdot amu^{-1}$	Vibration type
1	1313.38	1.64419	asym. bending
2	1313.61	1.6422	asym. bending
3	1314.1	1.6484	asym. bending
4	1531.00	27.4565	sym. bending
5	1531.09	27.449	sym. bending
6	3019.41	145.177	sym. stretching
7	3150.24	62.8181	asym. stretching
8	3150.27	62.8724	asym. stretching
9	3150.79	62.8305	asym. stretching

In contrast to the IR spectrum, both the symmetric bending and stretching modes are Raman-active. The symmetric stretching mode shows the highest Raman intensity among all vibrational modes, indicating that it is most prominent mode to be observed in a Raman spectrum.

3.2 Chloromethane

3.2.1 IR

The simulated vibrational modes of methane are summarized in Table 3 with the corresponding wavenumber, intensity and vibration type of each mode.

Tab. 3: Listed are the simulated wavenumbers and intensities of the vibrational modes of CH_3Cl.

Mode	Wavenumber $\tilde{\nu}$ / cm^{-1}	Intensity / km mol^{-1}	vibration type
1	725.98	23.93	C−Cl stretching
2	1010.21	3.13	rocking
3	1010.42	3.11	rocking
4	1361.61	14.72	scissoring
5	1455.99	6.46	twisting
6	1456.14	6.47	twisting
7	3057.12	21.81	sym. stretching
8	3170.28	6.28	asym. stretching
9	3170.74	6.27	asym. stretching

The table shows that all types of vibrations are IR active but the C−Cl stretching mode as well as the scissoring mode and symmetrical stretching mode are the most intense ones.

3.2.2 Raman

The simulated Raman-active vibrational modes of methane are summarized in Table 4 with the corresponding wavenumber, Raman intensity and vibration type of each mode.

Tab. 4: Listed are the simulated Raman shifts and intensities of the vibrational modes of CH_3Cl.

Mode	Raman Shift $\Delta\tilde{\nu}$ / cm^{-1}	Raman intensity / $Å^4$ amu^{-1}	vibration type
1	725.96	12.69	C−Cl stretching
2	1008.86	6.56	rocking
3	1010.02	6.53	rocking
4	1361.35	3.48	scissoring
5	1455.81	16.49	twisting
6	1456.34	16.50	twisting
7	3056.94	134.62	sym. stretching
8	3169.78	66.78	asym. stretching
9	3170.01	66.72	asym. stretching

The comparison to the IR table shows that all vibrational modes are also raman active but the most intense ones are now the stretching modes, with the symmetrical stretching being the most prominent one.

3.3 Dichloromethane

3.3.1 IR

The measured IR spectrum of dichloromethane is shown in Figure 4, plotting the intensity of the absorption against the wavenumber $\tilde{\nu}$.

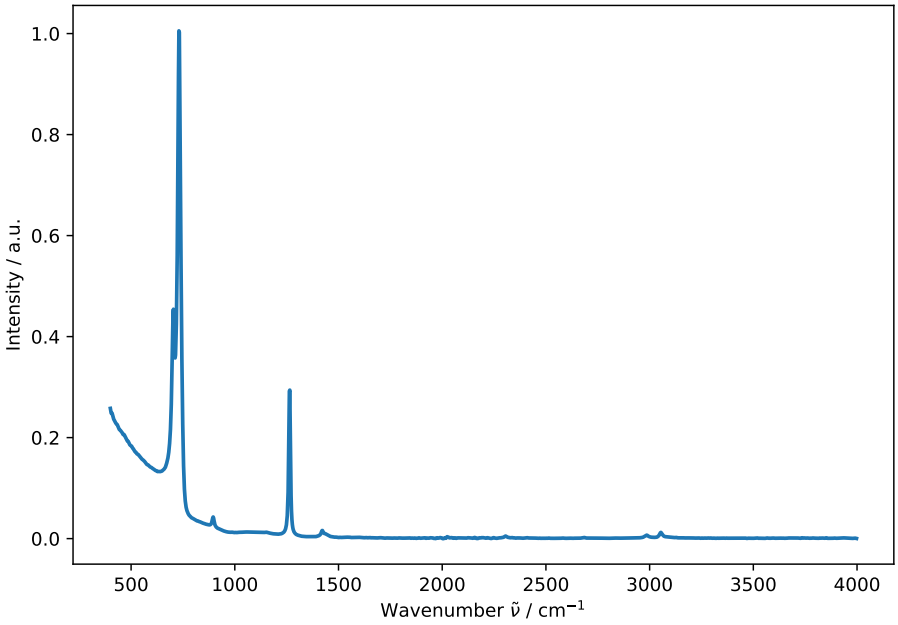

Fig. 4: Measured IR spectrum of dichloromethane.

By visual inspection of the IR spectrum in Figure 4, five absorption signals can be identified, which are listed with their corresponding wavenumbers and intensities in Table 5.

Tab. 5: Listed are the measured wavenumbers and intensities of the IR signals of CH_2Cl_2 with the corresponding type of the vibrational mode.

Signal	Wavenumber $\tilde{\nu}$ / cm^{-1}	Intensity / a.u.	Vibration type
1	704.00	0.45	C−Cl sym. stretching
2	730.53	1.01	C−Cl asym. stretching
3	895.82	0.04	rocking
4	1265.17	0.29	wagging
5	1422.29	0.02	scissoring

The simulated vibrational modes of dichloromethane are summarized in Table 6 with the corresponding wavenumber, intensity and vibration type of each mode.

Tab. 6: Listed are the simulated wavenumbers and intensities of the IR signals of CH_2Cl_2 with the corresponding type of the vibrational mode.

Mode	Wavenumber $\tilde{\nu}$ / cm^{-1}	Intensity / $KM \cdot mol^{-1}$	Vibration type
1	277.23	0.64	-
2	703.86	14.19	C−Cl sym. stretching
3	733.80	137.83	C−Cl asym. stretching
4	889.17	1.20	rocking
5	1153.54	0.00	-
6	1272.86	41.21	wagging
7	1441.46	0.01	scissoring
8	3107.43	9.81	sym. stretching
9	3194.30	0.64	asym. stretching

As can be seen in Table 6, the most intense IR-active modes are found at wavenumbers of 733.80 cm^{-1} and 1272.86 cm^{-1}, which correspond well to the measured signals at 730.53 cm^{-1} for the asymmetric stretching mode and 1265.17 cm^{-1} for the wagging mode in Figure 4. The C-H stretching modes at around 3100 cm^{-1} calculated by ORCA are barely visible in Figure 4.

3.3.2 Raman

The measured Raman spectrum of dichloromethane is shown in Figure 5, plotting the Raman intensity against the Raman shift $\Delta\tilde{\nu}$.

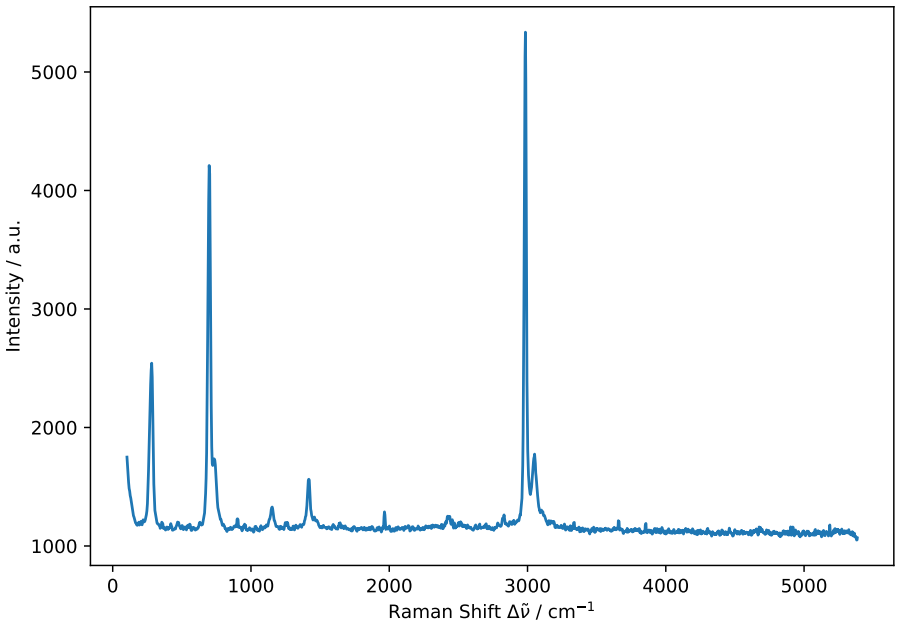

Fig. 5: Measured raman spectrum of dichloromethane.

By visual inspection of the Raman spectrum in Figure 5, five primary absorption signals can be identified, which are listed with their corresponding Raman shift, Raman intensity and vibration type of each mode.

Tab. 7: Listed are the measured Raman shifts and intensities of the signals of CH_2Cl_2.

Signal	Raman shift $\Delta\tilde{\nu}$ / cm^{-1}	intensity / a.u.	Vibration type
1	281.99	2542.67	C−Cl scissoring
2	697.77	4210.67	C−Cl sym. stretching
3	1418.07	1563.33	scissoring
4	2984.85	5336.00	sym. stretching
5	3051.13	1775.33	asym. stretching

The simulated Raman-active vibrational modes of dichloromethane are summarized in Table 8 with the corresponding Raman shift, Raman intensity and vibration type of each mode.

Tab. 8: Listed are the simulated Raman shifts and intensities of the vibrational modes of CH_2Cl_2.

Mode	Raman Shift $\Delta\tilde{\nu}$ / cm^{-1}	Raman intensity / $Å^4$ amu^{-1}	Vibration type
1	277.06	6.83	C−Cl scissoring
2	703.48	12.27	C−Cl sym. stretching
3	732.67	5.02	C−Cl asym. stretching
4	888.90	3.13	-
5	1153.83	11.78	-
6	1272.67	3.01	-
7	1441.64	12.42	scissoring
8	3106.65	108.70	sym. stretching
9	3193.09	62.65	asym. stretching

As can be seen in Table 7, the most intense Raman-active modes are found at wavenumbers of 281.99 cm^{-1}, 697.77 cm^{-1} and 2984.85 cm^{-1}, which correspond to the calculated signals at 277.06 cm^{-1} for the scissoring mode and 703.48 cm^{-1} for the symmetric stretching mode in Table 8. But similar to the IR spectrum, the wavenumbers of the C-H stretching modes in the measured Raman spectrum at 2984.85 cm^{-1} and 3051.13 cm^{-1} deviate by approximately 130 cm^{-1} from the calculated values of 3106.65 cm^{-1} and 3193.09 cm^{-1}.

3.4 Dibromomethane

3.4.1 IR

The measured IR spectrum of dibromomethane is shown in Figure 6, plotting the intensity of the absorption against the wavenumber $\tilde{\nu}$.

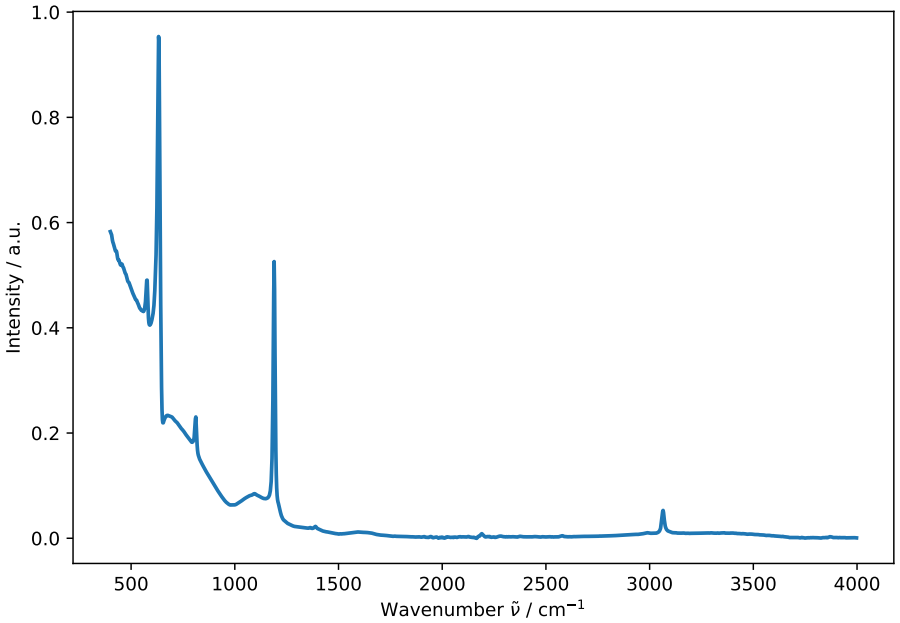

Fig. 6: Measured IR spectrum of dibromomethane.

By visual inspection of the IR spectrum in Figure 6, six absorption signals can be identified, which are listed with their corresponding wavenumbers and intensities in Table 9.

Tab. 9: Listed are the measured wavenumbers and intensities of the IR signals of CH_2Br_2.

Signal	Wavenumber $\tilde{\nu}$ / cm^{-1}	Intensity / a.u.	vibration type
1	455.05	0.52	-
2	577.49	0.49	C−Br sym. stretching
3	632.58	0.95	C−Br asym. stretching
4	677.48	0.23	-
5	812.16	0.23	rocking
6	1095.80	0.08	twisting
7	1189.66	0.53	wagging
8	1389.64	0.02	scissoring
11	3064.97	0.05	-

The simulated vibrational modes of dibromomethane are summarized in Table 10 with the corresponding wavenumber, intensity and vibration type of each mode.

Tab. 10: Listed are the simulated wavenumbers and intensities of the vibrational modes of CH_2Br_2.

Mode	Wavenumber $\tilde{\nu}$ / cm^{-1}	Intensity / $KM{\cdot}mol^{-1}$	vibration type
1	168.72	0.08	C−Br scissoring
2	573.58	4.08	C−Br sym. stretching
3	628.31	98.95	C−Br asym. stretching
4	806.07	4.64	rocking
5	1101.92	0.00	twisting
6	1205.80	65.32	wagging
7	1412.95	0.00	scissoring
8	3126.16	1.92	sym. stretching
9	3221.84	1.28	asym. stretching

As Table 10 shows, the most intense IR-active modes are found at wavenumbers of 628.31 cm^{-1} and 1205.80 cm^{-1}, which correspond well to the measured signals at 632.58 cm^{-1} for the C−Br asymmetric stretching mode and at 1189.66 cm^{-1} for the wagging mode. The comparison of the two tables also shows that although the twisting mode and scissoring mode should not be IR-active they still show up in the spectrum.

3.4.2 Raman

The measured Raman spectrum of dibromomethane is shown in Figure 7, plotting the Raman intensity against the Raman shift $\Delta\tilde{\nu}$.

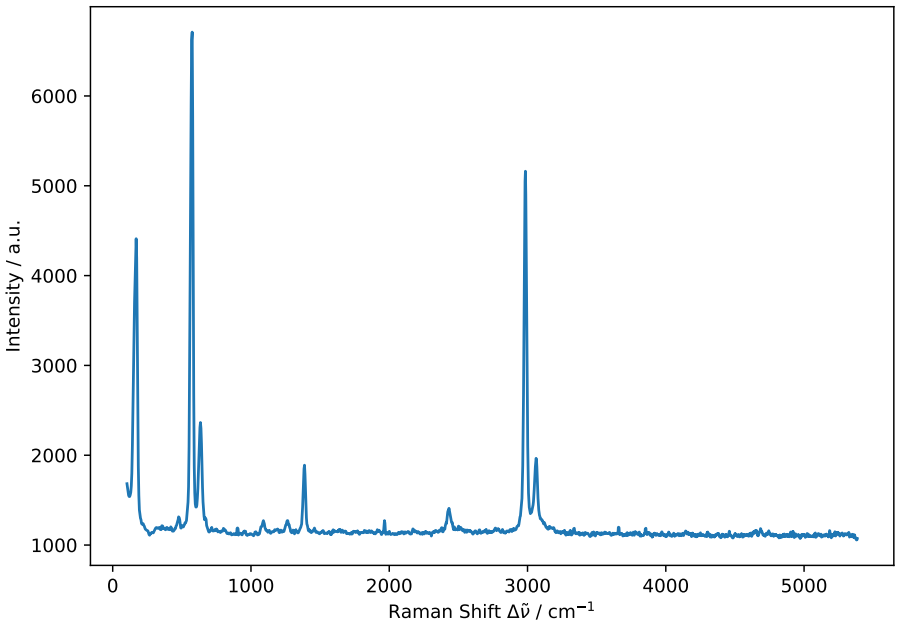

Fig. 7: Measured raman spectrum of dibromomethane.

By visual inspection of the Raman spectrum in Figure 7, seven primary absorption signals can be identified, which are listed with their corresponding Raman shift, Raman intensity and vibration type of each mode.

Tab. 11: Listed are the measured Raman shifts and intensities of the signals of CH_2Br_2.

Signal	Raman shift $\Delta\tilde{\nu}$ / cm^{-1}	Intensity / a.u.	vibration type
1	169.61	4410.67	C−Br scissoring
2	574.79	6711.00	C−Br sym. stretching
3	634.60	2364.33	C−Br asym. stretching
4	1387.16	1889.33	scissoring
5	2432.07	1409.00	-
6	2984.85	5162.00	sym. stretching
7	3062.11	1965.67	asym. stretching

The simulated Raman-active vibrational modes of dibromomethane are summarized in Table 12 with the corresponding Raman shift, Raman intensity and vibration type of each mode.

Tab. 12: Listed are the simulated wavenumbers and raman intensities of the vibrational modes of CH_2Br_2.

Mode	Wavenumber $\tilde{\nu}$ / cm^{-1}	Raman intensity / $Å^4$ amu^{-1}	vibration type
1	168.56	5.37	C−Br scissoring
2	574.64	13.43	C−Br sym. stretching
3	629.71	5.36	C−Br asym. stretching
4	806.60	2.41	rocking
5	1102.17	8.43	twisting
6	1205.71	0.74	wagging
7	1413.22	13.77	scissoring
8	3125.63	97.24	sym. stretching
9	3221.31	58.05	asym. stretching

As Table 12 shows, the most intense Raman-active modes are found at wavenumbers of 3125.63 cm^{-1} and 3221.31 cm^{-1}, which correspond to the measured signals at 2984.85 cm^{-1} for the symmetric stretching mode and at 3062.11 cm^{-1} for the asymmetric stretching mode. That means that the symmetric and asymmetric stretching of the C−H bonds is the most Raman-active type of vibration.

3.5 Chloroform

3.5.1 IR

The measured IR spectrum of chloroform is shown in Figure 8, plotting the intensity of the absorption against the wavenumber $\tilde{\nu}$.

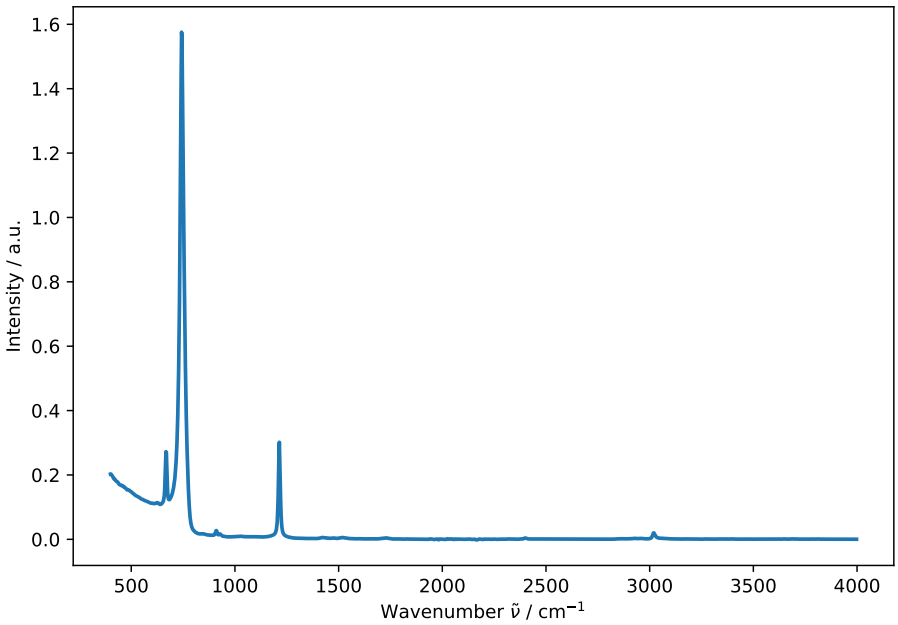

Fig. 8: Measured IR spectrum of chloroform.

By visual inspection of the IR spectrum in Figure 8, three absorption signals can be identified, which are listed with their corresponding wavenumbers and intensities in Table 13.

Tab. 13: Listed are the measured wavenumbers and intensities of the IR signals of $CHCl_3$.

Signal	Wavenumber $\tilde{\nu}$ / cm^{-1}	Intensity / a.u.	vibration type
1	626.46	0.11	-
2	667.27	0.27	C−Cl sym. stretching
3	742.78	1.58	C−Cl asym. stretching
4	910.10	0.03	-
5	928.47	0.02	-
6	1214.15	0.30	bending
7	3020.07	0.02	sym. stretching

The simulated vibrational modes of chloroform are summarized in Table 14 with the corresponding wavenumber, intensity and vibration type of each mode.

Tab. 14: Listed are the simulated wavenumbers and intensities of the vibrational modes of $CHCl_3$.

Mode	Wavenumber $\tilde{\nu}$ / cm^{-1}	Intensity / $KM \cdot mol^{-1}$	vibration type
1	254.78	0.06	C−Cl scissoring
2	254.97	0.06	C−Cl scissoring
3	362.33	0.46	C−Cl scissoring
4	665.85	7.26	C−Cl sym. stretching
5	741.92	167.74	C−Cl asym. stretching
6	742.13	167.67	C−Cl asym. stretching
7	1220.08	22.80	bending
8	1220.17	22.76	bending
9	3169.43	0.22	sym. stretching

As Table 14 shows, the most intense IR-active modes are found at wavenumbers of 741.92 cm^{-1} and 742.13 cm^{-1}, which correspond to the measured signal at 742.78 cm^{-1} for the C−Cl asymmetric stretching mode. That means that the asymmetric stretching of the C−Cl bond is the most IR active type of vibration. It is to be noted, that the simulation showed two distinct vibrational modes, while the measurement only shows one mode. The simulated bending modes at 1220.08 cm^{-1} and 1220.17 cm^{-1} that show the second highest intensities, were also measured as only one signal at 1214.15 cm^{-1}.

3.5.2 Raman

The measured Raman spectrum of chloroform is shown in Figure 9, plotting the Raman intensity against the Raman shift $\Delta\tilde{\nu}$.

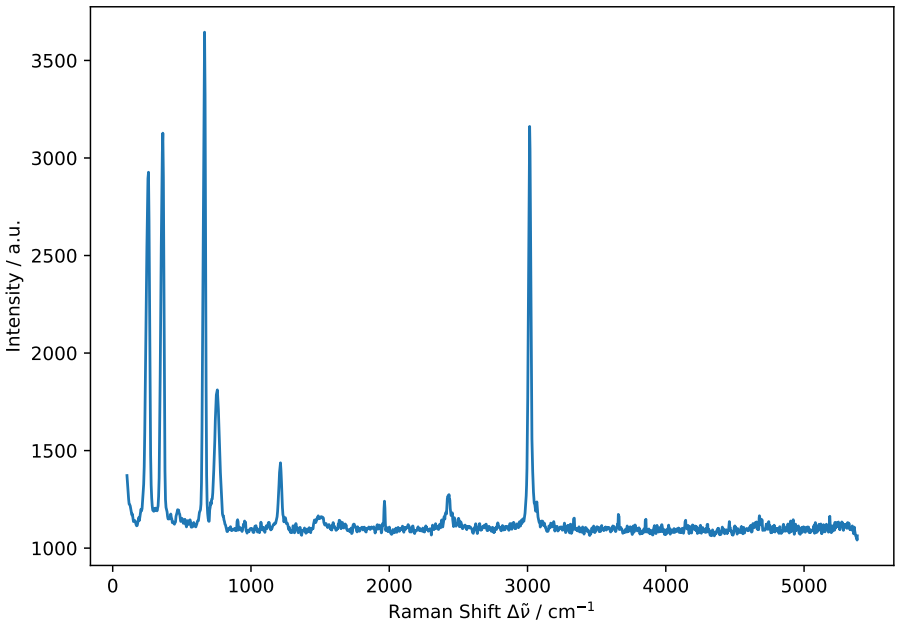

Fig. 9: Measured raman spectrum of chloroform.

By visual inspection of the Raman spectrum in Figure 9, six primary absorption signals can be identified, which are listed with their corresponding Raman shift, Raman intensity and vibration type of each mode.

Tab. 15: Listed are the measured Raman shifts and intensities of the signals of $CHCl_3$.

Signal	Raman shift $\Delta\tilde{\nu}$ / cm^{-1}	Intensity / a.u.	vibration type
1	258.84	2927.00	C−Cl scissoring
2	362.65	3127.33	C−Cl scissoring
3	664.38	3645.00	C−Cl sym. stretching
4	756.86	1811.33	C−Cl asym. stretching
5	1213.44	1437.33	bending
6	3015.32	3161.67	sym. stretching

The simulated Raman-active vibrational modes of tetrachloroethylene are summarized in Table 16 with the corresponding Raman shift, Raman intensity and vibration type of each mode.

Tab. 16: Listed are the simulated wavenumbers and Raman intensities of the vibrational modes of $CHCl_3$.

Mode	Wavenumber $\tilde{\nu}$ / cm^{-1}	Raman intensity / $Å^4$ amu^{-1}	vibration type
1	254.60	5.14	C−Cl scissoring
2	255.07	5.13	C−Cl scissoring
3	362.22	8.69	C−Cl scissoring
4	665.69	9.80	C−Cl sym. stretching
5	740.88	3.08	C−Cl asym. stretching
6	741.45	3.07	C−Cl asym. stretching
7	1220.22	6.04	bending
8	1220.68	6.05	bending
9	3168.77	77.28	sym. stretching

As Table 16 shows, the most intense Raman-active mode is found at the wavenumber 3168.77 cm^{-1}, which corresponds to the measured signal at 3015.32 cm^{-1} for the symmetric stretching mode. That means that the symmetric stretching of the C−H bond is the most Raman active type of vibration. Even though the C−Cl vibrational modes should not be nearly as intense as the symmetric stretching mode, they almost equal the simulated values.

3.6 Deuterated Chloroform

3.6.1 IR

The simulated vibrational modes of deuterated chloroform are summarized in Table 17 with the corresponding wavenumber, intensity and vibration type of each mode.

Tab. 17: Listed are the simulated wavenumbers and intensities of the vibrational modes of $CDCl_3$.

Mode	Wavenumber $\tilde{\nu}$ / cm^{-1}	Intensity / KM·mol^{-1}	vibration type
1	253.69	0.06	C−Cl scissoring
2	253.88	0.06	C−Cl scissoring
3	360.12	0.50	C−Cl scissoring
4	646.14	6.66	C−Cl sym. stretching
5	717.83	125.46	C−Cl asym. stretching
6	717.98	125.28	C−Cl asym. stretching
7	909.65	63.16	bending
8	909.66	63.19	bending
9	2342.61	0.74	sym. stretching

As Table 17 shows, the most intense IR-active modes are found at wavenumbers of 717.83 cm^{-1} for the C−Cl asymmetric stretching mode and 717.98 cm^{-1} for the second

C−Cl asymmetric stretching mode. Both of them correspond to the simulateded signals of chloroform at 741.92 cm^{-1} for the C−Cl asymmetric stretching mode and at 742.13 cm^{-1} for the second C−Cl asymmetric stretching mode. That means that the asymmetric stretching of the C−Cl bond is the most IR active type of vibration.

3.6.2 Raman

The measured Raman spectrum of deuterated chloroform is shown in Figure 10, plotting the Raman intensity against the Raman shift $\Delta\tilde{\nu}$.

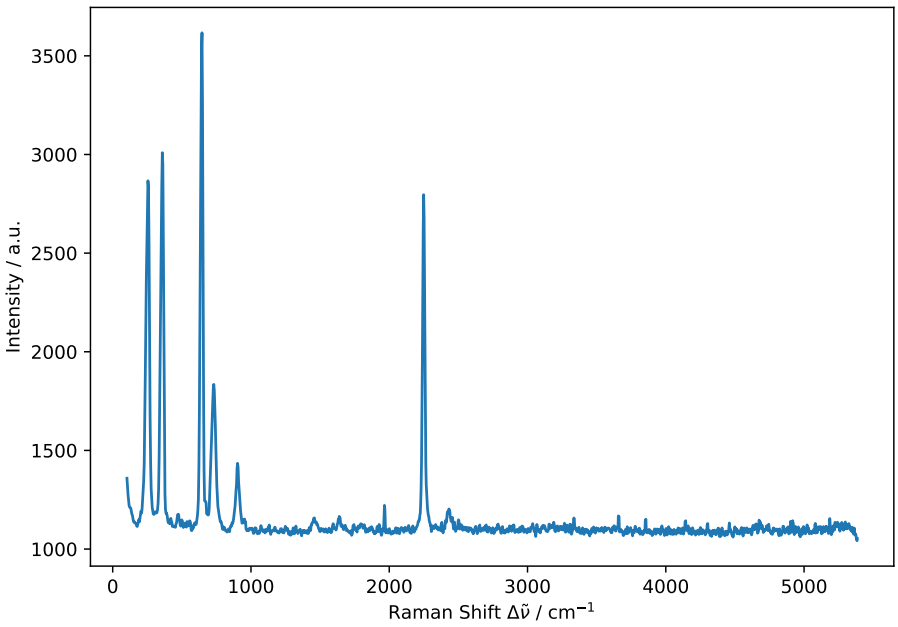

Fig. 10: Measured Raman spectrum of deuterated chloroform.

By visual inspection of the Raman spectrum in Figure 10, six primary absorption signals can be identified, which are listed with their corresponding Raman shift, Raman intensity and vibration type of each mode.

Tab. 18: Listed are the measured Raman shifts and intensities of the signals of $CDCl_3$.

Signal	Raman shift $\Delta\tilde{\nu}$ / cm^{-1}	Intensity / a.u.	vibration type
1	254.97	2866.67	C−Cl scissoring
2	358.83	3009.00	C−Cl scissoring
3	645.78	3616.67	C−Cl sym. stretching
4	731.05	1834.67	C−Cl asym. stretching
5	903.05	1434.67	bending
6	2248.93	2796.00	sym. stretching

The simulated Raman-active vibrational modes of deuterated chloroform are summarized in Table 19 with the corresponding Raman shift, Raman intensity and vibration type of each mode.

Tab. 19: Listed are the simulated wavenumbers and Raman intensities of the vibrational modes of $CDCl_3$.

Mode	Wavenumber $\tilde{\nu}$ / cm^{-1}	Raman intensity / $Å^4$ amu^{-1}	vibration type
1	253.69	0.06	C−Cl scissoring
2	253.88	0.06	C−Cl scissoring
3	360.12	0.50	C−Cl scissoring
4	646.14	6.66	C−Cl sym. stretching
5	717.83	125.46	C−Cl asym. stretching
6	717.98	125.28	C−Cl asym. stretching
7	909.65	63.16	bending
8	909.66	63.19	bending
9	2342.61	0.74	sym. stretching

As Table 19 shows, the most intense Raman-active modes are found at wavenumbers 717.83 cm^{-1} and 717.98 cm^{-1}, which correspond to the measured signal at 731.05 cm^{-1} for the C−Cl asymmetric stretching mode. It is to be noted that the two distinct vibrational modes shown in the simulation merge into one single mode in the measurement.

3.7 Tetrachloromethane

3.7.1 IR

The simulated vibrational modes of tetrachloromethane are summarized in Table 20 with the corresponding wavenumber, intensity and vibration type of each mode.

Tab. 20: Listed are the simulated wavenumbers and intensities of the vibrational modes of CCl_4.

Mode	Wavenumber $\tilde{\nu}$ / cm^{-1}	Intensity / KM·mol^{-1}	vibration type
1	212.71	0.00	scissoring
2	212.89	0.00	scissoring
3	310.72	0.06	scissoring
4	310.82	0.06	scissoring
5	310.88	0.06	scissoring
6	451.20	0.00	sym. stretching
7	754.80	185.52	asym. stretching
8	755.02	185.61	asym. stretching
9	755.51	185.58	asym. stretching

As Table 20 shows, the most intense IR-active modes are found at wavenumbers of 754.80 cm^{-1}, 755.02 cm^{-1} and 755.51 cm^{-1} for the C−Cl asymmetric stretching modes. It is to be noted, that the asymmetric stretching modes are the only IR-active modes.

3.7.2 Raman

The measured Raman spectrum of tetrachloromethane is shown in Figure 11, plotting the Raman intensity against the Raman shift $\Delta\tilde{\nu}$.

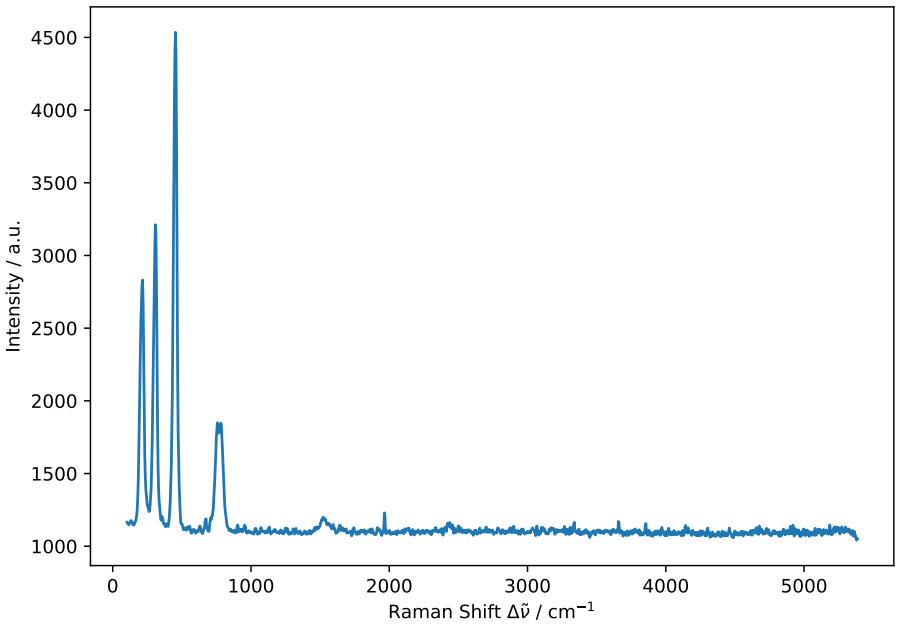

Fig. 11: Measured Raman spectrum of tetrachloromethane.

By visual inspection of the Raman spectrum in Figure 11, four primary absorption signals can be identified, which are listed with their corresponding Raman shift, Raman intensity and vibration type of each mode.

Tab. 21: Listed are the measured Raman shifts and intensities of the signals of CCl_4.

Signal	Raman shift $\Delta\tilde{\nu}$ / cm^{-1}	Intensity / a.u.	vibration type
1	216.25	2831.33	scissoring
2	308.95	3211.67	scissoring
3	454.10	4535.33	sym. stretching
4	756.86	1849.33	asym. stretching

The simulated Raman-active vibrational modes of tetrachloromethane are summarized in Table 22 with the corresponding Raman shift, Raman intensity and vibration type of each mode.

Tab. 22: Listed are the simulated wavenumbers and Raman intensities of the vibrational modes of CCl_4.

Mode	Wavenumber $\tilde{\nu}$ / cm^{-1}	Raman intensity / $Å^4$ amu^{-1}	vibration type
1	212.71	4.18	scissoring
2	212.91	4.17	scissoring
3	310.52	5.39	scissoring
4	310.84	5.40	scissoring
5	311.16	5.40	scissoring
6	451.08	16.40	sym. stretching
7	753.44	1.55	asym. stretching
8	754.26	1.56	asym. stretching
9	754.60	1.54	asym. stretching

As Table 22 shows, the most intense Raman-active mode is found at the wavenumber 451.08 cm^{-1}, which corresponds to the measured signal at 454.10 cm^{-1} for the C−Cl symmetric stretching mode. That means that the symmetric stretching mode is the most IR-active vibrational mode in tetrachloromethane.

3.8 Tetrachloroethylene

3.8.1 IR

The measured IR spectrum of tetrachloroethylene is shown in Figure 12, plotting the intensity of the absorption against the wavenumber $\tilde{\nu}$.

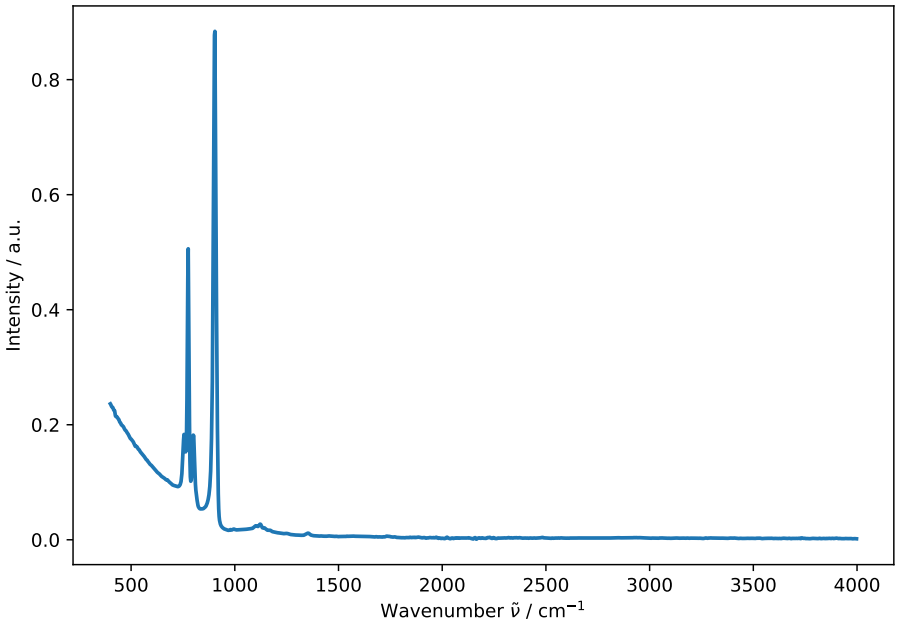

Fig. 12: Measured IR spectrum of tetrachloroethylene.

By visual inspection of the IR spectrum in Figure 12, six absorption signals can be identified, which are listed with their corresponding wavenumbers and intensities in Table 23.

Tab. 23: Listed are the measured wavenumbers and intensities of the IR signals of C_2Cl_4 with the corresponding type of the vibrational mode.

Signal	Wavenumber $\tilde{\nu}$ / cm^{-1}	Intensity / a.u.	Vibration type
1	755.02	0.18	-
2	775.42	0.51	asym. C-Cl stretching
3	799.91	0.18	-
4	903.98	0.88	asym. C-Cl stretching
5	1122.32	0.03	-
6	1354.95	0.01	-

The simulated vibrational modes of tetrachloroethylene are summarized in Table 24 with the corresponding wavenumber, intensity and vibration type of each mode.

Tab. 24: Listed are the simulated wavenumbers and intensities of the vibrational modes of C_2Cl_4.

Mode	Wavenumber $\tilde{\nu}$ / cm^{-1}	Intensity / KM·mol^{-1}	Vibration type
1	97.18	0.00	twisting
2	174.89	0.96	scissoring
3	234.77	0.00	scissoring
4	286.90	0.51	wagging
5	310.42	0.03	scissoring
6	342.99	0.00	asym. bending
7	447.02	0.00	sym. stretching
8	514.19	0.00	wagging
9	774.46	82.16	asym. stretching
10	895.52	202.05	asym. stretching
11	978.50	0.00	asym. stretching
12	1624.06	0.00	C = C stretching

As can be seen in Table 24, the most intense IR-active modes are found at wavenumbers of 774.46 cm^{-1} and 895.52 cm^{-1}, which correspond well to the measured signals at 755.02 cm^{-1} and 903.98 cm^{-1} in Figure 12. The signals at 755.02 cm^{-1} and 799.91 cm^{-1} can be assumed to occur due to isotopic effects, as chlorine has two stable isotopes, ^{35}Cl and ^{37}Cl, leading to small shifts in the vibrational frequencies. The two signals above 1100 cm^{-1} may indicate overtones or combination bands, which are weaker in intensity compared to the fundamental normal modes.

In comparison to the simulated IR spectrum of chloroform with the wavenumbers and vibrational modes in Table 13, tetrachloroethylene shows additional IR-active

modes in the low wavenumber region below 500 cm^{-1}, which can be attributed to the increased number of atoms in the molecule leading to more vibrational modes.

3.8.2 Raman

The measured Raman spectrum of tetrachloroethylene is shown in Figure 13, plotting the Raman intensity against the Raman shift $\Delta\tilde{\nu}$.

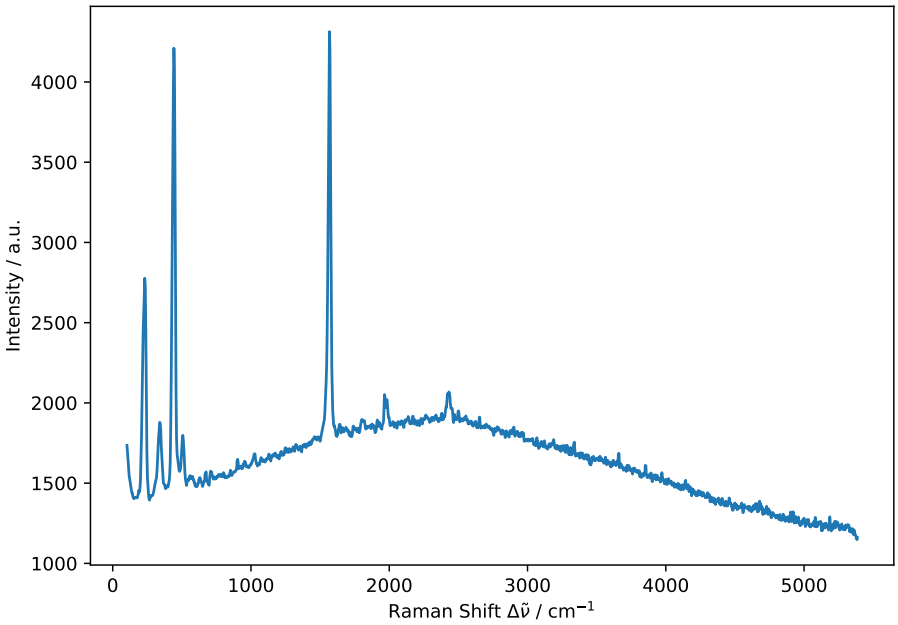

Fig. 13: Measured Raman spectrum of tetrachloroethylene.

By visual inspection of the Raman spectrum in Figure 13, six primary absorption signals can be identified, which are listed with their corresponding Raman shift, Raman intensity and vibration type of each mode.

Tab. 25: Listed are the measured Raman shifts and intensities of the signals of C_2Cl_4.

Signal	Raman shift $\Delta\tilde{\nu}$ / cm^{-1}	Intensity / a.u.	Vibration type
1	231.76	2776.67	scissoring
2	339.67	1879.00	asym. bending
3	442.71	4210.33	sym. stretching
4	1567.61	4313.00	C = C stretching
5	2432.07	2068.33	-

The simulated Raman-active vibrational modes of tetrachloroethylene are summarized in Table 26 with the corresponding Raman shift, Raman intensity and vibration type of each mode.

Tab. 26: Listed are the simulated wavenumbers and Raman intensities of the vibrational modes of C_2Cl_4.

Mode	Wavenumber $\tilde{\nu}$ / cm^{-1}	Raman intensity / $Å^4$ amu^{-1}	Vibration type
1	97.98	0.00	twisting
2	174.79	0.00	scissoring
3	234.62	5.56	scissoring
4	289.22	0.00	wagging
5	310.02	0.00	scissoring
6	342.83	4.61	asym. bending
7	446.81	15.61	sym. stretching
8	517.38	3.22	wagging
9	774.24	0.00	asym. stretching
10	895.62	0.00	asym. stretching
11	978.54	0.44	asym. stretching
12	1623.90	48.63	C = C stretching

In comparison to the simulated IR-active modes in Table 24, Table 26 shows that the most intense Raman-active mode is found at a wavenumber of 1623.90 cm^{-1}, which can be assigned to the C = C stretching mode of tetrachloroethylene, which has an intensity of 0 $KM{\cdot}mol^{-1}$ in the simulated IR spectrum, indicating that it is not IR-active. The cause for this lies in the rule of mutual exclusion, which applies to molecules with a center of symmetry, such as the inversion center of tetrachloroethylene. According to this rule, vibrational modes that are Raman-active are IR-inactive and vice versa, explaining the absence of the 1623.90 cm^{-1} mode in the IR spectrum.
By comparing the simulated Raman modes of C_2Cl_4 from Table 26 with the simulated Raman modes of $CHCl_3$ in Table 15, the structural differences between the two molecules can be explained. While both molecules show Raman-active modes in the low wavenumber region below 500 cm^{-1}, tetrachloroethylene shows an additional strong Raman-active mode at 1623.90 cm^{-1}, which can be attributed to the presence of the C = C double bond in C_2Cl_4 that is absent in $CHCl_3$. Additionally, the C-H stretching mode at 3168.77 cm^{-1} present in chloroform is not observed in tetrachloroethylene due to the lack of hydrogen atoms in its structure.

4 Discussion and Calculations

By plotting the calculated Raman shifts against the vibrational mode number for Methane and all Chloromethanes from Table 2, Table 4, Table 8, Table 16 and Table 22, the Raman trends of the investigated molecules can be visualized in Figure 14.

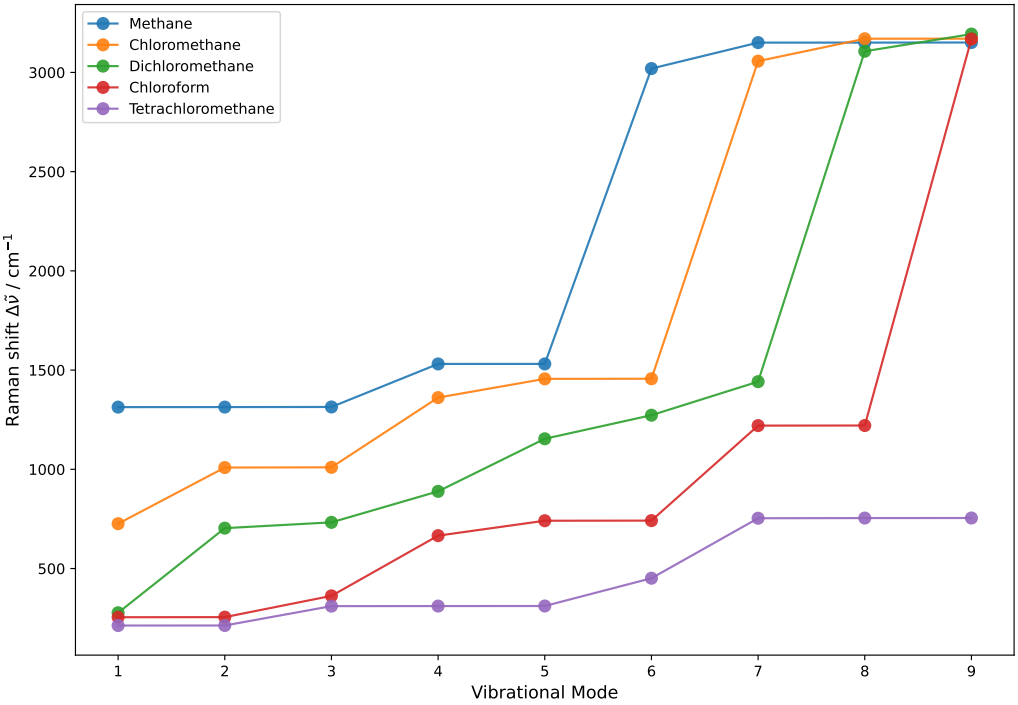

Fig. 14: Raman shifts plotted against the vibrational mode number for CH_4, CH_3Cl, CH_2Cl_2, $CHCl_3$ and CCl_4.

The first trend noticeable in Figure 14 is the decrease of the Raman shifts with increasing number of chlorine atoms in the molecule. This can be explained by the increasing reduced mass μ of the molecules according to Equation 4 due to the substitution of hydrogen atoms (m = 1 u) with chlorine atoms (m = 35.5 u). The increasing reduced mass μ leads to lower vibrational frequencies ν and wavenumbers $\tilde{\nu}$ according to Equation 3 and Equation 6.

$$\nu = \tilde{\nu} \cdot c \tag{6}$$

Following that argumentation, the number of vibrational modes at around 3000 cm^{-1}, which can be assigned to the C-H stretching vibrations, decreases with increasing number of chlorine atoms in the molecule until no C-H stretching modes are present in tetrachloromethane due to the absence of hydrogen atoms in its structure. In return, new vibrational modes appear in the low wavenumber region below 1000 cm^{-1}, which can be assigned to the C-Cl stretching vibrations. Another trend observable in Figure 14 is that methane and tetrachloromethane show more vibrational modes with nearly the same Raman shift compared to the other chloromethanes. This can be explained by the high symmetry of both molecules, which belong to the tetrahedral point group T_d. This trend is especially visible in the triply degenerate asymmetric stretching vibration of methane at 3150 cm^{-1} and tetrachloromethane at 754 cm^{-1}.

The Raman signal of the asymmetric C-H stretching vibration of dibromomethane at 3062.11 cm^{-1} in Table 11 shows a higher Raman shift and Raman intensity than

the corresponding signal of dichloromethane at 3051.13 cm^{-1} in Table 7. The higher Raman intensity can be explained by the higher polarizability of the electrons in bromine atoms compared to chlorine atoms, leading to a larger change in polarizability during the vibration and thus a stronger Raman signal.

For the comparison of the C−Cl and C−Br force constants, the reduced masses μ for both bonds are calculated using Equation 4.

$$\mu_{\mathrm{C-Cl}} = \frac{12\,\frac{\mathrm{g}}{\mathrm{mol}} \cdot 35.5\,\frac{\mathrm{g}}{\mathrm{mol}}}{12\,\frac{\mathrm{g}}{\mathrm{mol}} + 35.5\,\frac{\mathrm{g}}{\mathrm{mol}}} = 8.97\,\frac{\mathrm{g}}{\mathrm{mol}}$$

$$\mu_{\mathrm{C-Br}} = \frac{12\,\frac{\mathrm{g}}{\mathrm{mol}} \cdot 79.9\,\frac{\mathrm{g}}{\mathrm{mol}}}{12\,\frac{\mathrm{g}}{\mathrm{mol}} + 79.9\,\frac{\mathrm{g}}{\mathrm{mol}}} = 10.43\,\frac{\mathrm{g}}{\mathrm{mol}}$$

By rearranging Equation 3 and inserting ν from Equation 6 the force constant k can be calculated with Equation 7.

$$k = (2\pi \cdot \nu)^2 \cdot \mu = (2\pi \cdot \tilde{\nu} \cdot c)^2 \cdot \mu \tag{7}$$

By inserting the calculated reduced masses as well as the measured frequencies the force constants can be calculated.

$$\begin{aligned} k_{\mathrm{C-Cl}} &= \left(2\pi \cdot 703.86\,\mathrm{cm}^{-1} \cdot 2.99 \cdot 10^{10}\,\frac{\mathrm{cm}}{\mathrm{s}}\right)^2 \cdot 8.97\,\frac{\mathrm{g}}{\mathrm{mol}} \\ &= 1.568 \cdot 10^{29}\,\frac{\mathrm{g}}{\mathrm{mol} \cdot \mathrm{s}} \end{aligned}$$

$$\begin{aligned} k_{\mathrm{C-Br}} &= \left(2\pi \cdot 577.49\,\mathrm{cm}^{-1} \cdot 2.99 \cdot 10^{10}\,\frac{\mathrm{cm}}{\mathrm{s}}\right)^2 \cdot 10.43\,\frac{\mathrm{g}}{\mathrm{mol}} \\ &= 1.228 \cdot 10^{29}\,\frac{\mathrm{g}}{\mathrm{mol} \cdot \mathrm{s}} \end{aligned}$$

The comparison of the two force constants show that the C−Cl bond is stronger than the C−Br bond. That was to be expected because the atomic radii of carbon and chlorine are closer to each other than those of carbon and bromine, which enables a stronger bond. But it is to be noted that the approximation of the bond as a spring connecting the two atoms has some limitations, because it doesn't take things like electron clouds between the atoms into account.

The comparison of the raman spectra of deuterated chloroform and chloroform showed that the absorption signals of chloroform are generally located at higher wavenumbers than the signals of deuterated chloroform. This is most noticable for the signals of the symmetric stretching mode which is located at 3015.32 cm^{-1} for chloroform and at 2248.93 cm^{-1} for deuterated chloroform. This can be explained by using a simplified version of Hooke's law from Equation 3, which is defined as:

$$\nu = \sqrt{\frac{k}{\mu}}$$

It can be assumed, that the force constants of the C−H and C−D bonds is identical, which means the wavenumbers of the vibrations direcly correlate to the reduced masses. Those can be calculated by using **??**.

$$\mu_{\mathrm{C-H}} = \frac{12\,\frac{\mathrm{g}}{\mathrm{mol}} \cdot 1\,\frac{\mathrm{g}}{\mathrm{mol}}}{12\,\frac{\mathrm{g}}{\mathrm{mol}} + 1\,\frac{\mathrm{g}}{\mathrm{mol}}} = 0.923\,\frac{\mathrm{g}}{\mathrm{mol}}$$

$$\mu_{\mathrm{C-D}} = \frac{12\,\frac{\mathrm{g}}{\mathrm{mol}} \cdot 2\,\frac{\mathrm{g}}{\mathrm{mol}}}{12\,\frac{\mathrm{g}}{\mathrm{mol}} + 2\,\frac{\mathrm{g}}{\mathrm{mol}}} = 1.714\,\frac{\mathrm{g}}{\mathrm{mol}}$$

The calculation shows, that the reduced mass of the C−D bond is bigger than that of the C−H bond. That shows that due to the antiproprtional relationship between the reduced mass and the frequency, the wavenumber of the C−H vibration is bigger than that of the C−D vibration.

5 Conclusion

In this experiment, the vibrational modes of various chloromethanes, dibromomethane and tetrachloroethylene were investigated using IR and Raman spectroscopy. The measured IR spectra of dichloromethane, dibromomethane, chloroform and tetrachloroethylene were compared to simulated spectra obtained by calculations using the `ORCA` software. The measured Raman spectra of dichloromethane, dibromomethane, chloroform, deuterated chloroform, tetrachloromethane and tetrachloroethylene were also compared to simulated spectra. Additionaly the force constants of the C−Cl bond of dichloromethane was calculated as $1.568 \cdot 10^{29}\,\frac{\mathrm{g}}{\mathrm{mol \cdot s}}$ and compared to that of the C−Br bond of dibromomethane, which was calculated as $1.228 \cdot 10^{29}\,\frac{\mathrm{g}}{\mathrm{mol \cdot s}}$. Lastly the reduced masses of the C−H bond in chloroform and the C−D bond in deuterated chloroform were calculated and used to show the dependence of wavenumbers on the reduced masses.

6 References

[1] H. Dilger, *2025-pc2-script-en*, **2025**.